Int J Adv Manuf Technol (2017) 92:4161–4168
DOI 10.1007/s00170-017-0513-9

ORIGINAL ARTICLE

Process optimization and performance evaluation on laser beam welding of austenitic/martensitic dissimilar materials

W. W. Zhang[1] · **S. Cong**[1]

Received: 2 January 2017 / Accepted: 2 May 2017 / Published online: 12 May 2017
© Springer-Verlag London 2017

Abstract Laser beam welding of austenitic/martensitic dissimilar combination is used in a precision electromechanical product for function design. In order to achieve the better mechanical performance and physical performance of welding joints, process optimization was first carried out according to the Box-Behnken design method, and mathematical response models of weld depth and peak temperature value at special point were developed by multivariate quadratic/linear regression analysis. An optimal group of welding process parameters is obtained. Then, mechanical performance was evaluated by micro-structure analysis, non-destructive test, and uniaxial tensile test, and the influence of cooling style after laser beam welding process was discussed on hardness distribution and fracture force. It is shown that a rapid cooling style can avoid the crack occurrence at the heat-affected zone of austenitic stainless steel and enhance fracture force of weld joint. However, the hardness distribution is not even, and it has the highest value at the heat-affected zone of martensitic stainless steel and the lowest value at the heat-affected zone of austenitic stainless steel. However, the welding joint has a better mechanical performance under the condition of low temperature.

Keywords Laser beam welding · Response surface methodology · Non-destructive evaluation · Dissimilar materials

✉ W. W. Zhang
zhangweiwei0509103@163.com

[1] Institute of Electronic Engineering, China Academy of Engineering Physics, Mianyang 621900, China

1 Introduction

In order to take advantage of each base material to realize the special performance and functionalities, laser beam welding of dissimilar steel including carbon steel, stainless steel, and high-strength steel is applied in various industries such as automotive, railway vehicle, aviation manufacturing, and precision electromechanical product [1]. Many researches have been conducted and focused on the process optimization of different welding processes using statistical and numerical approaches [2].

Dissimilar welding joints between carbon steel, stainless steel, high-strength steel, and Kovar alloy have been widely studied. Investigation on metallurgical and mechanical characterization of dissimilar laser beam welds between low-carbon and austenitic stainless steel sheets was carried out, and micro-hardness test and quasi-static tensile-shear test were performed [3]. It is also shown that the fusion zone size in the weaker sheet is the controlling factors to determinate the mechanical strength of dissimilar austenitic/ferritic laser spot welds. Hybrid laser welding of selective laser molten stainless steel was proposed, and the power and speed parameters were investigated [4]. The efficiency of the welding process is evaluated through the line energy input versus the weld molten area. Research on Nd:YAG laser beam welding of AISI 420 stainless steel to Kovar alloy was carried out, and the morphology of weld zone solidification was observed [5]. It is found that the shape of grains depends on temperature gradient, and the columnar grains would be created in the fusion boundary of AISI 420 stainless steel side toward weld zone with the increase of temperature gradient. An experiment was carried out on dissimilar butt laser beam welding between twinning-induced plasticity (TWIP) steels and dual-phase (DP) steels, and the base materials and weld joints were fully characterized by means of metallography, micro-hardness, and tensile tests [6]. The results show that the laser beam welding

of TWIP steel with DP steels is not recommended without the use of proper metal fillers. An experimental study of laser spot welding on stainless steel sheets was carried out to analyze the influence of process parameters on cross-sectional size and shape of the welded spot [7]. It is found that the penetration depth and bead width of the welded spot increase with the increase of laser energy and laser incident angle.

A statistical design of experiment (DOE) was used to optimize process parameters (laser power, welding speed, and focus length) of ferritic/austenitic dissimilar weld, and the Taguchi approach was used for the selected factors. Joint strength was determined using the notched-tensile strength (NTS) method [8]. It is shown that the ferritic/austenitic laser beam welded joints can be improved effectively by optimizing the input parameters by the Taguchi approach. Process parameter optimization for Nd/YAG laser beam welding of ferritic/austenitic stainless steels in a constrained fillet configuration was carried out, and response surface methodology was used to develop a set of mathematical models relating the welding parameters to each of the weld characteristics [9, 10]. It is shown that the weld bead characteristics are significantly affected by laser power, welding speed, and incident angle, and an optimal set of process parameters to obtain better welds is given. Ferritic AISI 430F and martensitic AISI 440C stainless steel shells were laser beam welded in constrained butt configuration, and the effects of different combination of incident angles and offsets have been studied, analyzing the following parameters of the fusion zone: cross-sectional geometry (resistance length and width at the free surface), melting ratio between the dissimilar steels, presence of surface cracks and relative dimensions, and ultimate shear strength of the welds [11]. It is experimentally proved that an empirical relationship between the shear strength of the weld and the configuration adopted during experiments can be found by using full factorial DOE. Process optimization of laser welding of DP/TRIP steel sheets by response surface methodology was carried out, and the influence of the welding parameters including laser power, welding speed, and focus position was discussed on weld bead profile and quality [12]. Finally, strong, efficient, and low-cost weld joints could be achieved using the optimum welding conditions. Similarly, an optimization of CO_2 laser welding by ANN and Taguchi algorithm integrated approach was carried out to find out the optimum levels of the welding speed, the laser power, and the focal position [13]. The optimal solution is valid in the ranges of the welding parameters used for training the neural networks.

Although researches on laser beam welding of dissimilar stainless steel have been widely proposed, at current state, the study on laser beam welding of austenitic/martensitic dissimilar materials is seldom reported. Owing to the high expansive coefficient and low thermal conductivity of austenitic stainless steel, there is a long time retention period in high temperature, which will promote the crack occurrence during solidification process at heat-affected zone. For the martensitic stainless steel, hardenability at the heat-affected zone will lead to significant residual stress and enhancing stress corrosion; hence, it needs a slow solidification process. Obviously, there is a significant process conflict between martensitic stainless steel and austenitic stainless steel.

In order to achieve the better performance, in this research, welding process optimization was first carried out to obtain the target weld depth and temperature distribution. Then, mechanical performance was evaluated by micro-structure analysis and non-destructive test, and the influence of cooling style after laser bean welding process was discussed on hardness distribution and fracture force. Finally, a better weld joint with acceptable mechanical properties is obtained.

2 Experimental setup

2.1 Product description

Figure 1 shows the schematic view of the asynchronous motor used in the precision electromechanical products, which contains the cylinder, end closure, track ring, coil, and rotor. The coil is winded around the track ring, and then, they are assembled into the cylinder. In order to ensure the connection strength under the condition of mechanical vibration, the cylinder and the end closure are welding assembled. Meanwhile, in order to maintain the physical properties of the track ring which is made of retentive alloy, it cannot suffer from high temperature caused by laser beam welding. Totally, in the welding process, the weld depth between cylinder and end closure is more than 0.6 mm, while the peak temperature at the track ring would be no more than 110 °C.

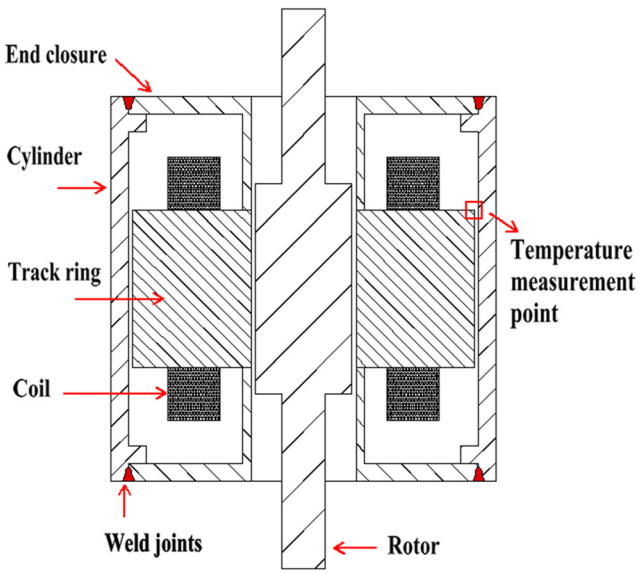

Fig. 1 Schematic view of the asynchronous motor

2.2 Process and equipment

From the viewpoint of function design, the material of cylinder and end closure is martensitic stainless steel SUS420J2 and austenitic stainless steel SUS303, respectively. Many welding methods can be used for connection process between cylinder and end closure such as arc welding, resistance welding, laser beam welding, and electron beam welding. In order to avoid welding distortion and significant residual stress during welding process, laser beam welding is used for the connection process between cylinder and end closure. Special features of the laser beam welding processes, resulting in very rapid introduction into various branches of industry, are the absence of direct contact between the heat and the welded surfaces, and also the possibility of controlling a wide range of heating conditions as a result of changes of radiation power, and the heat and light absorbing capacity of the welded materials.

In this research, Nd:YAG laser generator with the peak power 400 W was used for welding process of austenitic/martensitic stainless steel. As shown in Fig. 2, the specimen was fixed by three-jaw chuck, which has five-dimensional degree of freedom, namely moving or rotating in the X and Y direction to realize localization and rotating in the axial direction to realize welding. The variation of temperature at track ring during welding process was recorded by special thermal couple with high-speed data collection. The range of temperature measure is 50~200 °C, and the measure accuracy is 1%. The welding process is within the protective atmosphere of 99.9% nitrogen, and the weld depth is measured by microscopic analysis.

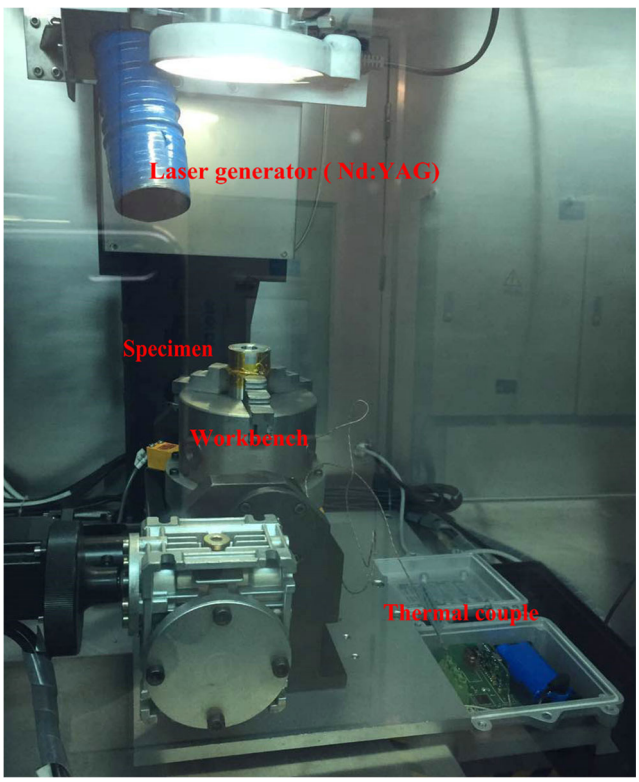

Fig. 2 Experimental setup of laser beam welding

3 Process parameter optimization for function design

In the viewpoint of connection strength, a larger weld depth is available for random vibration reliability. However, a larger weld depth depends on a strong power input, which will lead to a higher temperature distribution at the track ring and weaken the physical characteristic. It is a typical conflict between mechanical properties and physical properties. In order to obtain a suitable group of process parameters, process optimization can be carried out by response surface methodology.

3.1 Development of response surface methodology

Response surface methodology (RSM) is a collection of statistical method for designing experiments, developing models, evaluating the effects of factors, and searching for the optimal solution of the factors [14]. It has been widely used to set up the relationships of response values, and the essential input factors can be obtained. In this research, the weld depth and the peak temperature at the track ring were mainly focused, and the influence of laser beam welding parameters including power input, width of pulse, frequency, and welding speed was discussed on the weld depth and peak temperature. The mathematical respond models of peak temperature and weld depth can be expressed as follows:

$$T = g(f, \tau, P, v) \tag{1}$$

$$D = g'(f, \tau, P, v) \tag{2}$$

where f is the frequency of laser beam, τ is the width of pulse of laser beam, P is the power of laser beam, and v is the welding speed.

3.2 Box-Behnken design method

For the Nd:YAG laser generator, the laser beam is impulsive; hence, there is a relationship between the frequency of laser beam and welding speed. In order to maintain the performance of weld joints, the combination of frequency and welding speed should be within an acceptable range. In this research, the welding speed is constant, namely v = 60 mm/min.

A design of experiment such as the Box-Behnken design is implemented to estimate the response surface model. Three factors with three levels are coded and the corresponding forming parameters are shown in Table 1.

The design arrangement created by the software Minitab is shown in Table 2, and it also contains the experimental

Table 1 Parameters and their design levels

Variables	Levels		
	Low (−1)	Middle (0)	High (1)
f/Hz	15	20	25
τ/ms	3	4.5	6
P/W	90	110	130

response values. It should be paid attention that the central point is repeated three times to develop a higher prediction precision of the mathematical response model.

3.3 Determination of optimum process parameters

According to the variance analysis of the response values, the significance of possible mathematical regression model and the variables on the response value is evaluated. It is statistically proved that the mathematical response model of weld depth can be expressed by developing a multivariate quadratic regression model, while that of peak temperature can be written by developing a multivariate linear regression model. Owing to the evaluation of the significance of any term on the mathematical regression model by *F*-test, it is also statistically proved that the frequency of laser beam has no significance on the response values; hence, they will be ignored in the model. The modified model can be finally written as follows:

Table 2 Box-Behnken design matrix and results of experimental values

	Variables			Response values	
	f/Hz	τ/ms	*P*/W	*T*/°C	*D*/μm
1	15	3	110	92.0	380
2	25	3	110	93.1	358
3	15	6	110	118.4	258
4	25	6	110	120.3	283
5	15	4.5	90	81.6	173
6	25	4.5	90	80.3	166
7	15	4.5	130	137.9	690
8	25	4.5	130	142.7	719
9	20	3	90	74.4	206
10	20	6	90	109.4	143
11	20	3	130	116.0	854
12	20	6	130	156.6	567
13	20	4.5	110	99.8	308
14	20	4.5	110	94.4	335
15	20	4.5	110	97.6	305

Table 3 Possible solutions of process parameters

No.	Width of pulse/ms	Power/W	Weld depth/μm	Temperature/°C	Desirability
1	3.18	122.43	641	109.8	1.0
2	3.21	122.33	637	110.0	1.0

$$D = 1864.45 + 158.67\tau - 46.12P - 1.87\tau P + 0.31P^2 \quad (3)$$

$$T = -83.54 + 10.77\tau + 1.30P \quad (4)$$

In order to obtain a suitable group of process parameters, multi-objective design optimization (MDO) based on adaptive macro genetic algorithms (AMGA) was carried out to search the optimal design variables among the feasible regions. The multi-objective function containing the scope of weld depth and temperature is defined, and they must satisfy some constraint condition including scope of variables and maximum thinning. To summarize all design requirements, the objective function is defined as follows:

$$\begin{cases} \text{Object}: \ D \geq 0.6 \text{ mm and } T \leq 110\ ^{\circ}\text{C} \\ \text{Subject to}: \ 3 \text{ ms} \leq \tau \leq 6 \text{ ms} \quad 90 \text{ W} \leq P \leq 130 \text{ W} \end{cases} \quad (5)$$

According to the optimization calculation, as shown in Table 3, two sets of possible solution can be selected as the considered process parameters when the desirability is equal to 1.0. It should be paid attention that the desirability function analysis of the design variables among the feasible regions is shown in Fig. 3.

4 Performance evaluation of weld joints

The welding process optimization to realize mechanical properties and physical properties has been confirmed by the analysis mentioned above, and the welding process parameters are listed below: (1) width of pulse τ = 3.2 ms, (2) power input *P* = 122 W, (3) frequency of laser beam *f* = 20 Hz, and (4) welding speed *v* = 60 mm/min.

However, from the viewpoint of welding process of dissimilar materials, there is a significant conflict between martensitic stainless steel and austenitic stainless steel. For the martensitic stainless steel, hardenability at the heat-affected zone will lead to significant residual stress and enhancing stress corrosion; hence, a slow solidification is favorable for mechanical performance. For the austenitic stainless steel, the crack and coarse crystal easily occurs at the heat-affected zone; hence, a rapid solidification is favorable for mechanical performance. In order to maintain the performance of weld joints, the cooling air is used to control the micro-structure and connection strength.

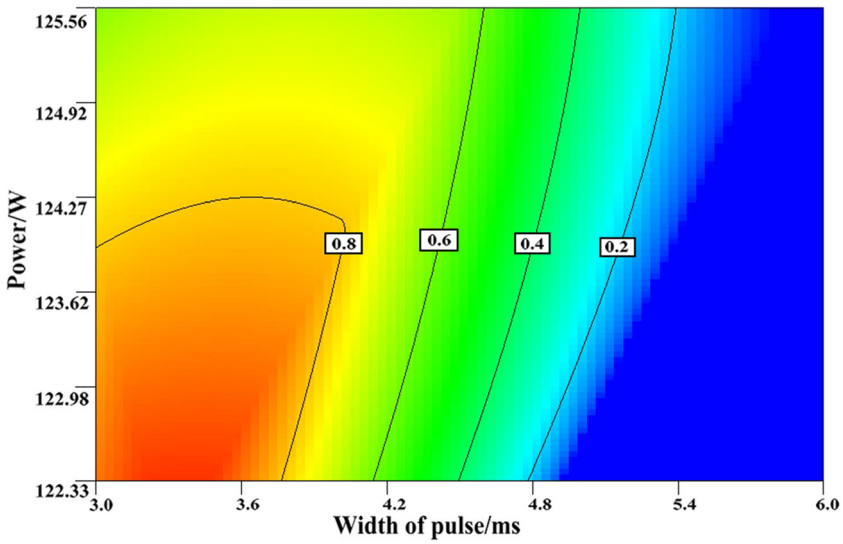

Fig. 3 Desirability function analysis

4.1 Defect evaluation

The defect evaluation of weld joints was carried out using pulse reflection method by sprinkler focused transducer in an incident angle. Figure 4a shows the schematic diagram of spraying water focused ultrasonic inspection method, and Fig. 4b shows the experimental setup. The specimen was fixed by three-jaw chuck, which can make the sample rotate by the controlled motor to realize circular inspection.

Figure 5 shows the echo waves of the inspection for austenitic/martensitic dissimilar stainless steel circular welds under the condition of different cooling styles. For the slow cooling style, it is shown that there is significant crack in the weld joints, which is represented by both the defect signal and the SEM images in Fig. 5a. Similarly, as shown in Fig. 5b, there is no crack in the weld joints for the rapid cooling style. It is experimentally proved that a rapid cooling style is beneficial for eliminating the crack at heat-affected zone.

4.2 Hardness profile

Figure 6 shows the hardness profile on the weld joints of austenitic/martensitic dissimilar materials under condition of different cooling rates. It can be seen that the hardness at the heat-affected zone of martensitic stainless steel is higher than that at other zone, while the hardness at the heat-affected zone of austenitic stainless steel is lower than that at other zone. According to the analysis of morphology images, the micro-structure at heat-affected zone of martensitic stainless steel is hybrid of martensite and austenite. However, compared with the slow cooling style, there will be a high proportion of martensite micro-structure under the condition of rapid cooling style, which causes a higher hardness. Similarly, the micro-structure at heat-affected zone of austenitic stainless steel is coarse crystal austenite. Compared with the slow cooling style, the growing up of coarse crystal will be restrained under the condition of rapid cooling style. It is experimentally

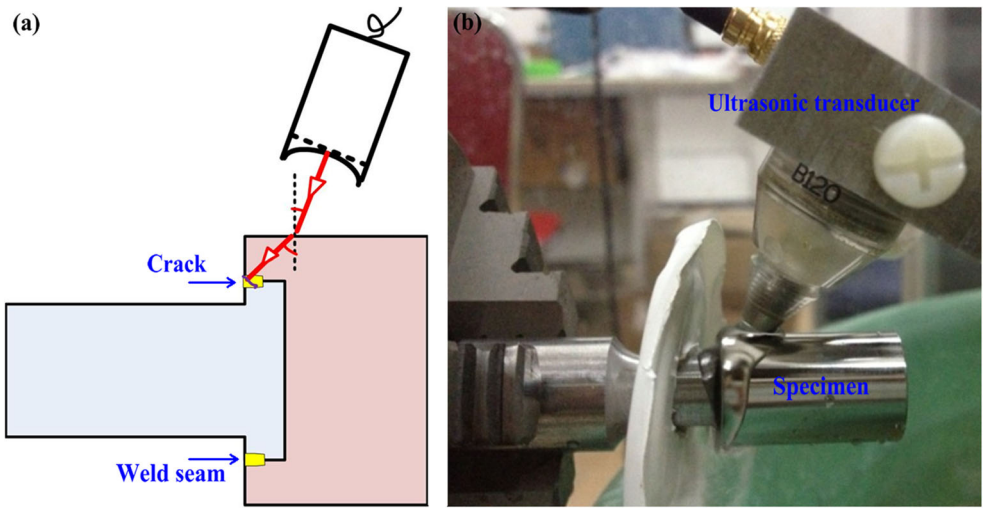

Fig. 4 Experimental setup of defect evaluation of weld joints. **a** Schematic diagram. **b** Experimental setup

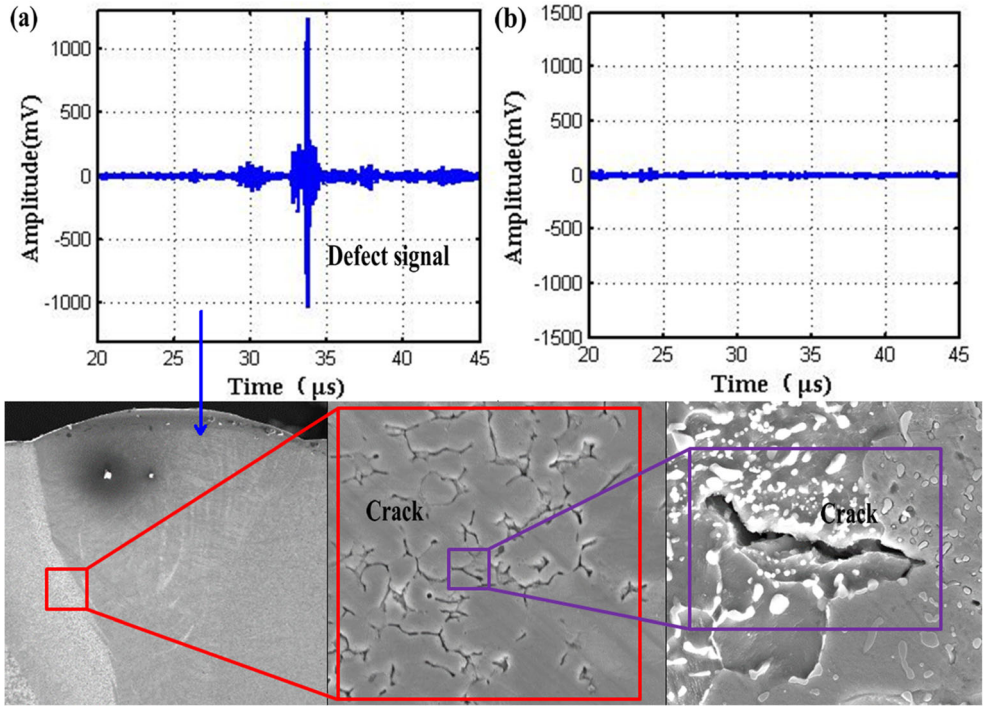

Fig. 5 Non-destructive evaluation of weld joints. **a** Slow cooling. **b** Rapid cooling

proved that the strength on the weld joints of dissimilar materials is uneven.

4.3 Mechanical performance at variable temperature

Figure 7 shows the mechanical performance of weld joints under different conditions. The specimen was designed to simulate the engineering application, and uniaxial tensile tests (simulate the shear performance of weld joints) were carried out to analyze the shear connection strength. It can be seen that the average fracture force of weld joints under the condition of slow cooling is 3.5 kN, while that under the condition of rapid cooling is increased to 7.5 kN. The fracture occurs at the heat-affected zone of austenitic stainless steel, and the fracture style is toughness according to the analysis of SEM images. It is well known that the crack possibly exists at the heat-affected zone of austenitic stainless steel and promotes the fracture.

Considering that the weld joints will suffer from vibration load, the random vibration test was applied to the product in a very wide frequency range. According to the GJB1027A-2005 test standard, the tests were conducted under the condition of 20~2000 Hz of frequency and 15 g of total root mean square acceleration. The results show that the average fracture force of specimen after random vibration test is not decreased, which means the weld joint has a high reliability.

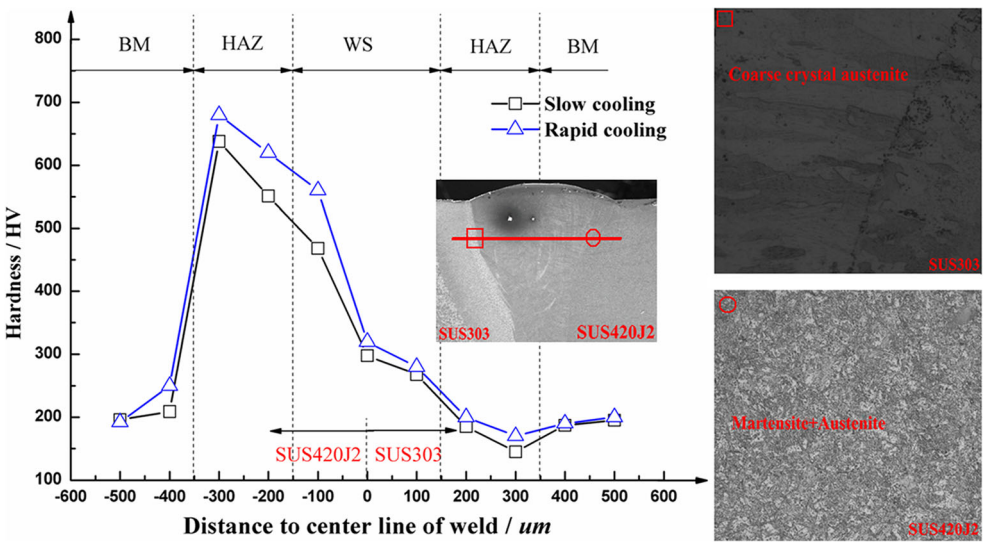

Fig. 6 Hardness profile and morphology images at heat-affected zone

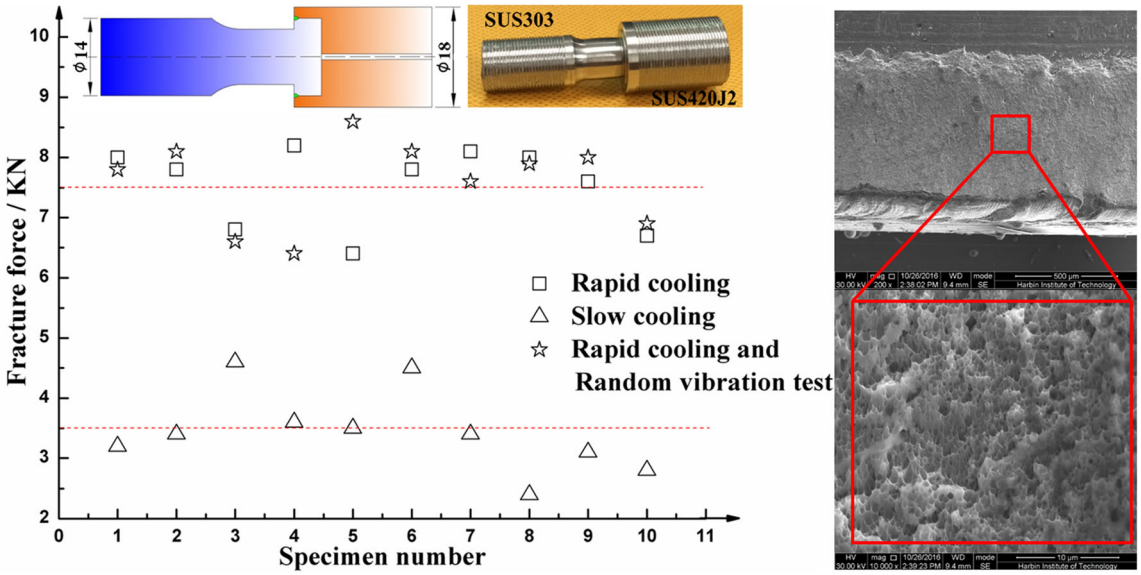

Fig. 7 Fracture force of weld joints under different conditions and the SEM fracture images

Owing to the complicated use conditions for the weld joints, the mechanical performance should be evaluated under the condition of variable temperature values including 60, 25, 0, −25, and −60 °C. As shown in Fig. 8, it can be seen that the fracture force has less variation when the temperature is up to 0 °C; however, the fracture force is significantly increased as the temperature is decreased to −25 °C. When the temperature is −60 °C, the fracture force is increased to 9.0 kN. The main reason of mechanical performance variation is that the microstructure is beginning to transform from austenitic to martensite when the temperature is below 0 °C. Hence, there will be better mechanical performance under the condition of low temperature.

5 Conclusion

Process optimization and performance evaluation of austenitic/martensitic dissimilar combination by laser beam welding have been conducted, the influence of welding process parameters was discussed on weld depth and peak temperature value at special point, and the influence of cooling style after laser beam welding process was discussed on hardness distribution and fracture force. The main conclusions are listed below:

1. According to the Box-Behnken design method, mathematical response models of weld depth and peak temperature value at special point were developed by multivariate

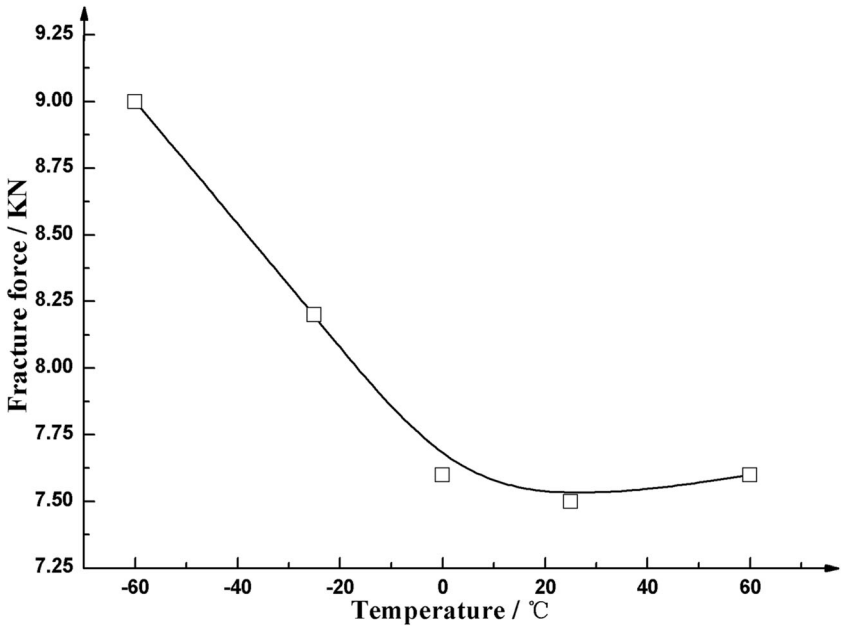

Fig. 8 Fracture force of weld joints at variable temperature values

quadratic/linear regression analysis, and an optimal group of welding process parameters including width of pulse τ = 3.2 ms, power input P = 122 W, frequency of laser beam f = 20 Hz, and welding speed v = 60 mm/min is obtained to realize the target weld depth (≥0.6 mm) and peak temperature (≤110 °C).
2. Mechanical performance was evaluated by micro-structure analysis, non-destructive test, and uniaxial tensile test, and a rapid cooling style can avoid the crack occurrence at the heat-affected zone of austenitic stainless steel and enhance fracture force of weld joint from 3.5 to 7.5 kN.
3. Hardness distribution is not even, and it has the highest value 680 HV at the heat-affected zone of martensitic stainless steel and the lowest value 200 HV at the heat-affected zone of austenitic stainless steel.
4. The welding joint has a better mechanical performance under the condition of low temperature. When the temperature value is decreased from 25 to −60 °C, the fracture force of weld joint is increased from 7.5 to 9.0 kN.

Acknowledgments This paper was financially supported by Major project of process improvement in China Academy of Engineering Physics (TA140401). The authors would like to take this opportunity to express their sincere appreciation.

Compliance with ethical standards

Competing interests The authors declare that they have no competing interests.

References

1. Eshtayeh MM, Hrairi M, AKM M (2016) Clinching process for joining dissimilar materials: state of the art. Int J Adv Manuf Technol 82(1–4):179–195
2. Benyounis KY, Olabi AG (2008) Optimization of different welding processes using statistical and numerical approaches—a reference guide. Adv Eng Softw 39(6):483–496
3. Torkamany MJ, Sabbaghzadeh J, Hamedi MJ (2012) Effect of laser welding mode on the microstructure and mechanical performance of dissimilar laser spot welds between low carbon and austenitic stainless steels. Mater & Des 34:666–672
4. Casalino G, Campanelli SL, Ludovico AD (2013) Laser-arc hybrid welding of wrought to selective laser molten stainless steel. Int J Adv Manuf Technol 68(1–4):209–216
5. Baghjari SH, SAA AM (2014) Experimental investigation on dissimilar pulsed Nd:YAG laser welding of AISI 420 stainless steel to kovar alloy. Mater & Des 57:128–134
6. Rossini M, Spena PR, Cortese L, Matteis P, Firrao D (2015) Investigation on dissimilar laser welding of advanced high strength steel sheets for the automotive industry. Mater Sci Eng A 628(1): 288–296
7. Liao YC, Yu MH (2007) Effects of laser beam energy and incident angle on the pulse laser welding of stainless steel thin sheet. J Mater Process Technol 190(1–3):102–108
8. Anawa EM, Olabi AG (2008) Optimization of tensile strength of ferritic/austenitic laser-welded components. Opt Lasers Eng 46(8): 571–577
9. MMA K, Romoli L, Fiaschi M, Dini G, Sarri F (2012) Multiresponse optimization of laser welding of stainless steels in a constrained fillet joint configuration using RSM. Int J Adv Manuf Technol 62(5–8):587–603
10. MMA K, Romoli L, Fiaschi M, Dini G, Sarri F (2012) Laser beam welding of dissimilar stainless steels in a fillet joint configuration. J Mater Proc Technol 212:856–867
11. Romoli L, CAA R (2015) The influence of laser welding configuration on the properties of dissimilar stainless steel welds. Int J Adv Manuf Technol 81(1–4):563–576
12. Reisgen U, Schleser M, Mokrov O, Ahmed E (2012) Optimization of laser welding of DP/TRIP steel sheets using statistical approach. Opt & Laser Tech 44(1):255–262
13. Olabi AG, Casalino G, Benyounis KY, MSJ H (2006) An ANN and Taguchi algorithms integrated approach to the optimization of CO2 laser welding. Adv Eng Softw 37(10):643–648
14. Zhang WW, Yuan SJ (2015) Pre-form design for hydro-forming process of combined ellipsoidal shells by response surface methodology. Int J Adv Manuf Technol 81(9–12):1977–1986